Modeling Response of Concrete Material due to Biaxial Loading using Finite Element Method Software Based

Data Iranata[1], Endah Wahyuni[1], Aniendhita Rizki Amalia[1], and Sylvya Anggraini[1]

Abstract— **Generally the concrete behavior can be observed by the experimental analysis. However, since the computer technology development has been increased rapidly, the computer simulations are also able to represent the detail behavior of concrete. This paper presents the modeling response of concrete material subjected to biaxial loading using finite element method software based. The plain concrete plates with dimensions 200mm x 200mm x 50mm and 150mm x 150mm x 50mm are analyzed using various combinations of biaxial loading. The results of the biaxial load combinations are covering the three non-linear regions of compression–compression, compression–tension, and tension–tension. The results of finite element analysis are also show good agreement to the experimental results that been taken from the previous study. The comparison results the difference between analytical and experimental study are less than 5%. Therefore, the concrete material model based on this finite element method software can be used to simulate the responses in the real condition.**

Keywords— **Concrete, Material, Biaxial, Finite Element Method Software Based**

I. Introduction

Generally, the understanding of the structural behaviour is obtained from the experimental research and studies. The experimental testing is very important in order to obtain the detail behaviour of the structural component which is based on the real condition. However, to obtain the detail and accurate experimental results it is also consuming significant efforts, time and funding. Until now, those are the major obstacle of the experimental research and studies.

Nowadays, advances in computer technology and numerical methods have allowed the simulation of engineering problems that traditionally have been addressed via experimentation and theoretical models. Some industries have been able to design sophisticated engineered systems based solely on computer simulation. In addition, many complex phenomena, such as airplane crashes and car accidents, can already be analyzed by computer simulations instead of the experimental testing.

In the context of structural engineering, using computer simulation to realistically represent the behaviour of structural systems in detail in various situations, such as the global response and the detailed damage to a structure during a severe loading, is also a goal which must be achieved by engineers.

One of the numerical methods that commonly able to perform the detail response of the structural component is using finite element method and analysis. The basic concept of finite element analysis is dividing the continuum element into several elements and connected of each others with nodal element. Each element also has several nodes which are also have appropriate degree of freedom.

In order to perform the detailed damage of the reinforced concrete structural component, the computer simulation of the concrete material basic response such as uniaxial and biaxial loading should be also presented with very well [1]. Therefore, this paper presents the computer modelling response of concrete material due to biaxial loading using finite element method software based. The behaviour of concrete material is simulated and verified with the experimental results that conduct by [2] and [3]. The linear as well as non-linear response of the concrete material model is simulate and observed to obtain the detail response of the concrete material model. Hence, the concrete material model based on this finite element method software can be used to simulate the responses in the real condition.

II. Concrete Material Properties Subjected to Biaxial Loading by Experimental Observation

Figure 1 show a typical biaxial strength envelops for concrete subjected to proportional biaxial loading. Experimental studies by [2] present concrete under conditions of biaxial compression shows values of increased compressive strength is up to about 1.25 f'_c. Another result of the investigation conducted by [3]

[1]Data Iranata, Endah Wahyuni, Aniendhita Rizki Amalia, and Sylvya Anggraini are with Departement of Civil Engineering, Faculty of Civil Engineering and Planning, Institut Teknologi Sepuluh Nopember, Surabaya, 60111.

E-mail : iranata_data@yahoo.com; endahwahyuni@gmail.com; aniendhita.ra@gmail.com; pie_sylvya@yahoo.com.

illustrates a failure surface that is slightly stronger than that developed by [2]. The maximum ratio of equibiaxial and uniaxial compressive yield stress is about 1.45 f'_c. The difference in the failure surfaces may be due to a number of factors such as rate of loading, conditions of the specimens during testing, preparation of the specimens, properties of the mixes or size effects. Research by [3] has propose that the discrepancies are due in part to differences in the type of coarse aggregate used in the two studies and in part to the use by [2] of a slower rate of loading than is currently standard. Under biaxial tension, concrete material reveals a constant tensile strength, compared with values obtained under uniaxial loading. Under combination of tension and compression, concrete material shows a noticeably reduced strength. For biaxial compression, concrete material exhibits an increased initial stiffness that may be attributed to the Poisson effect and an increased degree of ductility at the peak stress, which is an indication of the reduction in the degree of internal damage as compared to uniaxial loading, as shown in Figure 2 and Figure 3 as presented by [2] and [3] respectively.

III. Concrete Material Constitutive Model Development

Concrete can behave as either a linear or nonlinear material which is depending on the level and the nature of the stresses to which it is subjected. Under low levels of stress, concrete are able to behave as a linear elastic material, while for higher values of stress and for sustained loading it shows highly nonlinear properties which have a considerable effect on the behaviour of reinforced concrete structure.

In order to predict the concrete behavior, this study adopts the concrete damage plasticity model proposed by [4]. The damaged plasticity model constitutive is offered for the analysis of concrete material at low confining pressures. The damaged plasticity model for concrete material is based on the assumption of scalar isotropic damage and is designed for applications in which the concrete is subjected to arbitrary loading conditions, including cyclic loading. The model takes into consideration the degradation of the elastic stiffness induced by plastic straining both in tension as well as compression

A. Concrete Linear Elastic Material Model

Linear elasticity is the material model behaviour of the deformable solid objects which can be internally stressed due to prescribed loading conditions. Linear elasticity relies upon the continuum hypothesis and it is applicable in the macroscopic as well as microscopic length scales. Linear elasticity is a simplification of the general nonlinear theory of elasticity and is a branch of continuum mechanics. The fundamental assumptions of linear elasticity are the small deformations or strains, which usually less then 5%, and linear relationships between the components of stress and strain, as mentioned by [5]. In addition linear elasticity is only valid for stress states that do not produce yielding.

For elastic materials the Hooke's law represents the material behavior and relates the unknown stresses and strains. The general equation for Hooke's law is

$$\sigma ij = Cijkl\, \varepsilon kl \quad (1)$$

where $\sigma_{ij} = \sigma_{ji}$ is the total stress (Cauchy stress) tensor, $\varepsilon_{kl} = \varepsilon_{lk}$ is the total elastic strain, and $C_{ijkl} = C_{klij} = C_{jikl} = C_{ijlk}$ is the fourth-order elasticity tensor.

For an isotropic material the elasticity tensor has no preferred direction. It means an applied force will give the same displacements, which is relative to the direction of the force, no matter the direction in which the force is applied. Isotropic linear elasticity well approximates the behaviour of concrete material under tensile type of loading, including uniaxial and multiaxial tension. Before the peak stress state the stress-strain relation is almost linear up to the peak load in such a loading environment. This approximation also holds for the behavior under small compressive loading. However, this type of model becomes unacceptable as the applied compressive loads increase, as well as the concrete crushing occur.

In the isotropic linear elasticity, the elasticity tensor may be written as

$$C_{ijkl} = C_{pq} = \begin{bmatrix} C_{11} & C_{12} & C_{12} & 0 & 0 & 0 \\ C_{12} & C_{11} & C_{12} & 0 & 0 & 0 \\ C_{12} & C_{12} & C_{11} & 0 & 0 & 0 \\ 0 & 0 & 0 & \frac{C_{11}-C_{12}}{2} & 0 & 0 \\ 0 & 0 & 0 & 0 & \frac{C_{11}-C_{12}}{2} & 0 \\ 0 & 0 & 0 & 0 & 0 & \frac{C_{11}-C_{12}}{2} \end{bmatrix}$$

The Lamé constants can be expressed in terms of Young's modulus, E, and Poisson's ratio, v, as presented by [5]. In terms of E and v, the general equation of isotropic linear elasticity becomes:

$$\sigma_{ij} = \frac{Ev}{(1+v)(1-2v)}\delta_{ij}\varepsilon_{kk} + \frac{E}{(1+v)}\varepsilon_{ij} \quad (2)$$

where the factor 2 comes from the double optical path difference and n_{fiber} is the refractive index of a single mode SMF-28 fiber.

B. Concrete Damage Plasticity Material Model

The concrete damaged plasticity model is primarily intended to provide a general capability for the analysis of concrete material and/or structures under cyclic and/or dynamic loading. The model is also suitable for the analysis of other quasi-brittle materials, such as rock, mortar, cement paste and ceramics; but it is the behavior of concrete that is used in the remainder of this section to motivate different aspects of the constitutive theory. Under low confining pressures, concrete material behaves in a brittle manner; the main failure mechanisms are cracking in tension and crushing in compression. The brittle behavior of concrete disappears when the confining pressure is significantly large to prevent crack propagation. In these circumstances failure is driven by the consolidation and collapse of the concrete micro-porous microstructure, leading to a macroscopic response

that resembles that of a ductile material with work hardening, as mentioned by [4].

Modelling and simulating the concrete material behaviour under large hydrostatic pressures is out of the scope of the plastic-damage model considered here. The constitutive theory in this part aims to capture the effects of irreversible damage associated with the failure mechanisms that occur in concrete materials under fairly low confining pressures.

1) Concrete under Uniaxial Condition

It is assumed that the uniaxial stress-strain curves can be transformed into stress versus plastic strain curves of the form as follows:

$$\sigma_t = \sigma_t(\tilde{\varepsilon}_t^{pl}, \dot{\tilde{\varepsilon}}_t^{pl}) \quad (3)$$

$$\sigma_c = \sigma_c(\tilde{\varepsilon}_c^{pl}, \dot{\tilde{\varepsilon}}_c^{pl}) \quad (4)$$

where the subscripts t and c refer to tension and compression, respectively.

$\dot{\tilde{\varepsilon}}_t^{pl}$ and $\dot{\tilde{\varepsilon}}_c^{pl}$ are the equivalent plastic strain rates.

$$\tilde{\varepsilon}_t^{pl} = \int_0^t \dot{\tilde{\varepsilon}}_t^{pl}\, dt \quad (5)$$

and

$$\tilde{\varepsilon}_c^{pl} = \int_0^t \dot{\tilde{\varepsilon}}_c^{pl}\, dt \quad (6)$$

are the equivalent plastic strains.

Under uniaxial loading conditions the effective plastic strain rates are given as:

In uniaxial tension:

$$\dot{\tilde{\varepsilon}}_t^{pl} = \dot{\varepsilon}_{11}^{pl} \quad (7)$$

In uniaxial compression:

$$\dot{\tilde{\varepsilon}}_c^{pl} = -\dot{\varepsilon}_{11}^{pl} \quad (8)$$

As shown in Figure 4, when the concrete material specimen is unloaded from any point on the strain softening branch of the stress-strain curves, the unloading response is observed to be weakened and the elastic stiffness of the material appears to be damaged or degraded. The degradation of the elastic stiffness is significantly different between tension and compression testing, the effect is more pronounced as the plastic strain increases. The degraded response of concrete is characterized by two independent uniaxial damage variables, d_t and d_c, which are assumed to be functions of the plastic strains variables:

$$d_t = d_t(\tilde{\varepsilon}_t^{pl}), (0 \le d_t \le 1) \quad (9)$$

$$d_c = d_c(\tilde{\varepsilon}_c^{pl}), (0 \le d_c \le 1) \quad (10)$$

If E_0 is the initial (undamaged) elastic stiffness of the material, the stress-strain relations under uniaxial tension and compression loading are, respectively:

$$\sigma_t = (1 - d_t)E_0(\varepsilon_t - \tilde{\varepsilon}_t^{pl}) \quad (11)$$

$$\sigma_c = (1 - d_c)E_0(\varepsilon_c - \tilde{\varepsilon}_c^{pl}) \quad (12)$$

The effective uniaxial cohesion stresses are given as:

$$\bar{\sigma}_t = \frac{\sigma_t}{(1-d_t)} = E_0(\varepsilon_t - \tilde{\varepsilon}_t^{pl}) \quad (13)$$

$$\bar{\sigma}_c = \frac{\sigma_c}{(1-d_c)} = E_0(\varepsilon_c - \tilde{\varepsilon}_c^{pl}) \quad (14)$$

The effective uniaxial cohesion stresses are determining the size of the yield or failure surface.

2) Yield Condition

The plastic-damage concrete model uses a yield condition based on the yield function proposed by [6] and incorporates the modifications proposed by [7] to describe for different evolution of strength under tension and compression. In terms of effective stresses the yield function takes the form:

$$F(\bar{\sigma}, \tilde{\varepsilon}^{pl}) = \frac{1}{1-\alpha}\left(\bar{q} - 3\alpha\bar{p} + \beta(\tilde{\varepsilon}^{pl})(\hat{\bar{\sigma}}_{max}) - \gamma(\hat{\bar{\sigma}}_{max})\right) - \bar{\sigma}_c(\tilde{\varepsilon}_c^{pl}) \le 0 \quad (15)$$

in which $\bar{p}$ is the effective hydrostatic pressure, defined as:

$$\bar{p} = -\frac{1}{3}\bar{\sigma}: I \quad (16)$$

and $\bar{q}$ is the Mises equivalent effective stress, defined as:

$$\bar{q} = \sqrt{\frac{3}{2}(\bar{s}:\bar{s})} \quad (17)$$

where:

$$\bar{S} = \bar{\sigma} + \bar{p}I \quad (18)$$

are deviatoric part of the effective stress tensor $\bar{\sigma}$, $\hat{\bar{\sigma}}_{\max}$ is the algebraically maximum eigenvalue of $\bar{\sigma}$, I is the unit tensor, α and γ are dimensionless material constants.

The function $\beta(\tilde{\varepsilon}^{pl})$ is given as:

$$\beta(\tilde{\varepsilon}^{pl}) = \frac{\bar{\sigma}_c(\tilde{\varepsilon}_c^{pl})}{\bar{\sigma}_t(\tilde{\varepsilon}_t^{pl})}(1 - \alpha) - (1 + \alpha) \quad (19)$$

Where $\bar{\sigma}_t(\tilde{\varepsilon}_t^{pl})$ and $\bar{\sigma}_c(\tilde{\varepsilon}_c^{pl})$ is the tensile and compressive cohesion stress, respectively.

In biaxial compression, with $\hat{\bar{\sigma}}_{\max}$, Eq. (15) can be reduced into the well-known Drucker-Prager yield condition.

The coefficient α can be determined from the initial equibiaxial and uniaxial compressive yields stress, σ_{bo} and σ_{co}, respectively as:

$$\alpha = \frac{\sigma_{bo} - \sigma_{co}}{2\sigma_{bo} - \sigma_{co}} \quad (20)$$

Typically experimental values of the ratio σ_{bo}/σ_{co} for concrete are in the range from 1.10 to 1.20, yielding values of α between 0.08 and 0.12, as mentioned by [1].

The coefficient γ enters the yield function only for the stress states of triaxial compression, when $\hat{\bar{\sigma}}_{\max} < 0$. This coefficient can be determined by comparing the yield conditions along the tensile and compressive meridians. By definition, the Tensile Meridian (TM) is the locus of stress states satisfying the condition

$$\hat{\bar{\sigma}}_{\max} = \hat{\bar{\sigma}}_1 > \hat{\bar{\sigma}}_2 = \hat{\bar{\sigma}}_3 \quad (21)$$

and the Compressive Meridian (CM) is the locus of stress states such that

$$\hat{\bar{\sigma}}_{\max} = \hat{\bar{\sigma}}_1 = \hat{\bar{\sigma}}_2 > \hat{\bar{\sigma}}_3 \quad (22)$$

where $\hat{\bar{\sigma}}_1$, $\hat{\bar{\sigma}}_2$, and $\hat{\bar{\sigma}}_3$ are the eigenvalues of the effective stress tensor.

It can be easily shown that

$$(\hat{\bar{\sigma}}_{\max})_{TM} = \frac{2}{3}\bar{q} - \bar{p} \quad (23)$$

And

$$(\hat{\bar{\sigma}}_{\max})_{CM} = \frac{1}{3}\bar{q} - \bar{p} \quad (24)$$

along the tensile and compressive meridians, respectively. With $\hat{\bar{\sigma}}_{\max} < 0$ the corresponding yield conditions are presented as follows:

For Tensile Meridian (TM)

$$\left(\frac{2}{3}\gamma + 1\right)\bar{q} - (\gamma + 3\alpha)\bar{p} = (1-\alpha)\bar{\sigma}_c \quad (25)$$

For Compressive Meridian (CM)

$$\left(\frac{1}{3}\gamma + 1\right)\bar{q} - (\gamma + 3\alpha)\bar{p} = (1-\alpha)\bar{\sigma}_c \quad (26)$$

Let assumed $K_c = \frac{\bar{q}(TM)}{\bar{q}(CM)}$ for any given value of the hydrostatic pressure $\bar{p}$ with $\hat{\bar{\sigma}}_{\max} < 0$

Then:

$$K_c = \frac{\gamma+3}{2\gamma+3} \quad (27)$$

The coefficient γ is, therefore, evaluated as:

$$\gamma = \frac{3(1-K_c}{2K_c-1} \quad (28)$$

Research by [8] presents the ratio of the second stress invariant of the tensile meridian to the compressive meridian, K_C, are in the range from 0.5 to 1.0, which is most available experimental failure data are fitted just as well with straight as with curved meridian. A value of, K_C = 0.67 which is typical for concrete, gives γ = 3as mentioned by [4].

If $\hat{\bar{\sigma}}_{\max} < 0$, the yield conditions along the tensile and compressive meridians, respectively, reduce to:

$$\left(\frac{2}{3}\beta + 1\right)\bar{q} - (\beta + 3\alpha)\bar{p} = (1-\alpha)\bar{\sigma}_c \quad (29)$$

$$\left(\frac{1}{3}\beta + 1\right)\bar{q} - (\beta + 3\alpha)\bar{p} = (1-\alpha)\bar{\sigma}_c \quad (30)$$

Let $K_t = \frac{\bar{q}(TM)}{\bar{q}(CM)}$ for any given value of the hydrostatic pressure $\bar{p}$ with $\hat{\bar{\sigma}}_{\max} > 0$; then:

$$K_t = \frac{\beta+3}{2\beta+3} \quad (31)$$

Typical yield surfaces are shown in Figure 5 and Figure 6 for the deviatoric plane and for the plane-stress conditions, respectively.

3) Flow Rule

The plastic-damage model can be assumed as non-associated potential flow and it takes form as:

$$\dot{\varepsilon}^{pl} = \dot{\lambda}\frac{\partial G(\bar{\sigma})}{\partial \bar{\sigma}} \quad (32)$$

The flow potential *G* chosen for this model is the Drucker-Prager hyperbolic function as present as follows:

$$G = \sqrt{(\varepsilon\sigma_{t0})^2 + \bar{q}^2} - \bar{p}\tan\psi \quad (33)$$

Where:

ψ is the dilatation angle measures in the *p-q* plane at high confining pressure

σ_{t0} is the uniaxial tensile stress at failure

ε is a strain parameter

This flow potential, which is continuous and smooth, certifies that the flow direction is defined uniquely. The function asymptotically approaches the linear Drucker-Prager flow potential at high confining pressure stress and crosses the hydrostatic pressure axis at 90°

IV. Concrete Material Modeling and Simulation Method

A. Modelling Parameters

The following table present the modelling parameters based on the previous studies by [2] and [3]. The concrete strength and modulus of elasticity for previous research by [2] are 30.68 MPa and 32500 MPa, respectively. And for the previous study by [3], the concrete strength and modulus of elasticity are 37.60 MPa and 25000 MPa. The other material properties, such as concrete strength, concrete modulus of elasticity, dimension of specimen, and also biaxial loading ratio, which are related to the proposed modelling and simulation, are present in Table 1 and Table 2. The experimental results of previous studies are also being used to verify the proposed concrete material modelling response due to biaxial loading.

B. Concrete Material Modelling

This study present the finite element modelling for concrete material subjected to biaxial loading. The proposed model is presented in this study using finite element software based called ABAQUS. The input parameters for the proposed model are adopted and following the previous studies by [2] and [3]. In order to obtain the great accuracy, the input parameter should be exactly the same with the observed previous experimental studies.

Figure 7 present the geometric of the proposed model. Let assumed that the tension loading is in the positive direction. While the boundary conditions are assigned as three-dimension roller supports along at the corresponding *x* and *y* directions. Except for corner nodal, the boundary condition is assigned as hinged support. So, the translations on the *x*, *y*, and *z* are restrained in this nodal.

And for the concrete material nonlinear analysis, the proposed model is assigned using concrete damage plasticity model that built in the ABAQUS properties menu. Again, the input parameter are adopted and following the previous studies. The input parameters that applied in this study are presented in Table 3.

Another parameter that should be assigned is the element properties for the concrete model. Since this study using three dimensional analysis, the brick element is should be assigned in the proposed model. In order to maintain the accuracy of the proposed model, the quadratic element is preferred instead of the linear. Hence, in this paper, the concrete model is assigned using quadratic brick element with 20 nodes.

V. Results and Discussion

A. Concrete Model Subjected to Biaxial Compression Loading

The following table present simulation results of the proposed concrete material models subjected to biaxial compression loading compared with experimental results by [2]. Parameters that should be checked are stress and strain in the *1*, *2*, and *3* directions, which are related to the *x*, *y*, and *z* direction in the local axis. The simulation results show the good agreement between proposed model and the experimental results. The average discrepancies are about 5%. Except for the strain results in the *2* direction, the maximum discrepancy can be

reach about 29%. That error is happened due to the inconsistent Poisson's ratio value iteration condition at the nonlinear condition of the proposed concrete material model. The graphical result of the comparison between proposed models subjected to biaxial compressions with the experimental results by [2] is presented in the Figure 8. The strain results in the *1* and *2* directions generally show the good agreement both in the linear as well as non-linear condition. For the *3* direction the small discrepancies occur since the linear condition. The good agreements occur in the peak condition of ε_3. And in the post-peak condition the small discrepancies are happen again.

The other experimental results that used to verify the proposed model is presented by [3]. The simulation results of the proposed concrete material models subjected to biaxial compression loading compared with experimental results by [3] is presented in Table 5. Again, the simulation results show the good agreement between proposed model and the experimental results. The average discrepancies are about 10%. The maximum discrepancy is about 40% which occur in the *1* direction. Additionally, the graphical result of the comparison between proposed models subjected to biaxial compressions with the experimental results by [3] is presented in the Figure 9. The strain results show the good agreement in the linear condition. At the peak condition the significant discrepancies are occur in the both directions. The discrepancies that occur in the non-linear condition are happening usually due to the difficulty to achieve the convergence of the Newton-Raphson iteration. To solve those problems the refined model is necessary to be developed.

Figure 10 and 11 present the comparison ratio of biaxial and uniaxial compression between proposed models with the experimental results by [2] and [3], respectively. Comparisons between proposed models with the experimental by [2] generally show good agreement. Small discrepancies, which are less than 10%, still occur at the several conditions. Hence, the simulation results of the proposed are acceptable.

Comparisons between proposed models with the experimental by [3] that presented in Figure 11 also show very good agreement. In the most condition, the discrepancy between proposed model and experimental results are only about 2%. The maximum discrepancy that occurs is only about 5%, which happen in the condition of the ratio of biaxial and uniaxial compression are about 1.4. Based on this result, the proposed model can be used to simulate the response of the concrete material subjected to biaxial compression loading.

B. Concrete Model Subjected to Biaxial Tension Loading

The following table present simulation results of the proposed concrete material models subjected to biaxial tension loading compared with experimental results by [2]. The simulation results show the good agreement between proposed model and the experimental results, which is the average discrepancies are about 5%. The significant discrepancy is happen at the strain results in the *3* direction, which is can be reach about 22%. Again, the error is happened due to the inconsistent Poisson's ratio value iteration condition at the nonlinear condition of the proposed concrete material model. The graphical result of the comparison between proposed models subjected to biaxial compressions with the experimental results by [2] is presented in the Figure 12. The small discrepancy, which is about 10%, is happen along the linear condition at the both direction.

C. Concrete Model Subjected to Biaxial Compression and Tension Loading

The following table present simulation results of the proposed concrete material models subjected to biaxial compression and tension loading compared with experimental results by [2]. Again, the simulation results show the good agreement between proposed model and the experimental results, which is the average discrepancies are about 5%. The maximum discrepancy is happen at the strain results in the *2* direction, which is can be reach only about 9%. The graphical result of the comparison between proposed models subjected to biaxial compressions with the experimental results by [2] is presented in the Figure 13. The strain results show the good agreement in the linear condition. At the post-peak condition the small discrepancies are occur in the both directions. Based on this result, the proposed model can be used to simulate the response of the concrete material subjected to biaxial compression-tension loading.

VI. CONCLUSIONS

The proposed concrete material model subjected to biaxial loading has presented in this paper. The proposed model has performed using finite element method software based. The proposed model has also verified with experimental testing results by previous studies. The comparisons results show that the average discrepancies between proposed model and the experimental testing results are about 5%. Based on this result, the proposed model can be used to simulate the responses of the concrete material subjected to biaxial loading in the real condition.

REFERENCES

[1] H M Chen and D Iranata, "Realistic Simulation of Reinforced Concrete Structural Systems with Combine of Simplified and Rigorous Component Model," *Structural Engineering and Mechanics*, vol. 30, no. 5, pp. 619–645, November 2008.

[2] H Kupfer and H K Hubert, "Behaviour of Concrete Under Biaxial Stresses," *ACI Journal*, vol. 66, no. 8, pp. 656–666, January 1969.

[3] W S Yin, Eric C M Su, M A Mansur, and Thomas T C Hsu, "Biaxial Tests Of Plain And Fiber Concrete," *ACI Materials Journal*, vol. 86, no. 3, pp. 236-243, January 1989.

[4] W F Chen, E Yamaguchi, M D Kotsovos, and A D Pan, "Constitutive models," in *ASCE-ACI International Workshop of Finite Element Analysis of Reinforced Concrete Structures II*, New York, 1991, pp. 36-117.

[5] S P Timoshenko and J N Goodier, *Theory of Elasticity*, 3rd ed. New York, United States: McGraw-Hill, 1970.

[6] J Lubliner, J Oliver, S Oller, and E Onate, "A Plastic-Damage Model for Concrete," *International Journal of Solids and Structures*, vol. 25, no. 3, pp. 299-329, August 1989.

[7] J Lee and G L Fenves, "Plastic-Damage Model for Cyclic Loading of Concrete Structures," *Journal of Engineering Mechanics*, vol. 124, no. 8, pp. 892-900, August 1998.

[8] N S Ottosen, "A Failure Criterion for Concrete," *ASCE Journal of Engineering Mechanics Division*, vol. 103, no. 4, pp. 527-535, July/August 1977.

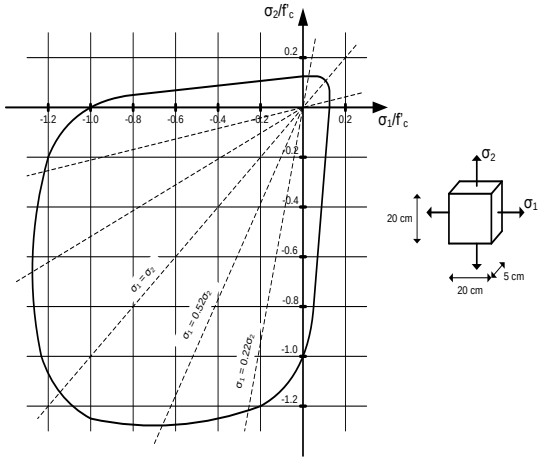

Figure 1: Biaxial strength of concrete as presented by [2].

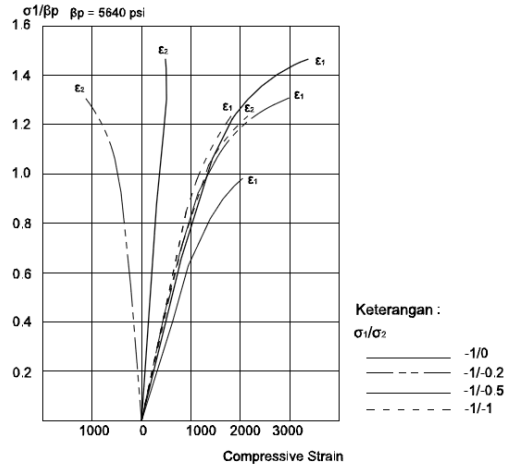

Figure 3: Stress-strain relationships of concrete under biaxial compression as presented by [3]

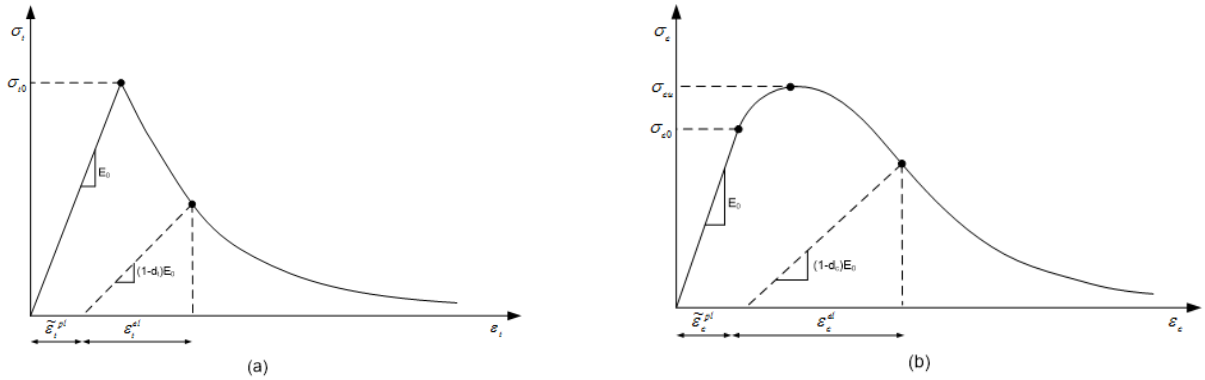

Figure 4: Response of concrete subjected to uniaxial loading: (a) tension loading and (b) compression loading, as presented by [4]

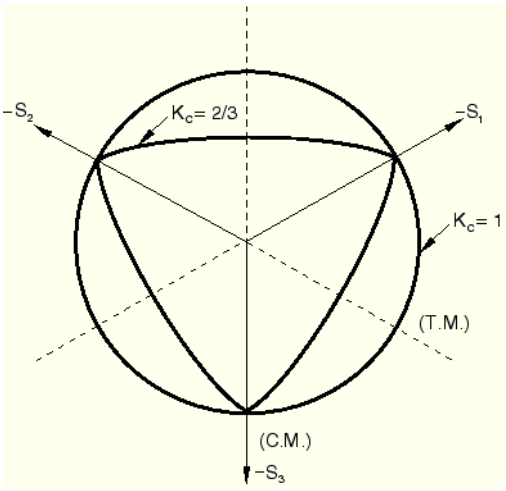

Figure 5: Yield surfaces in the deviatoric plane as presented by [4]

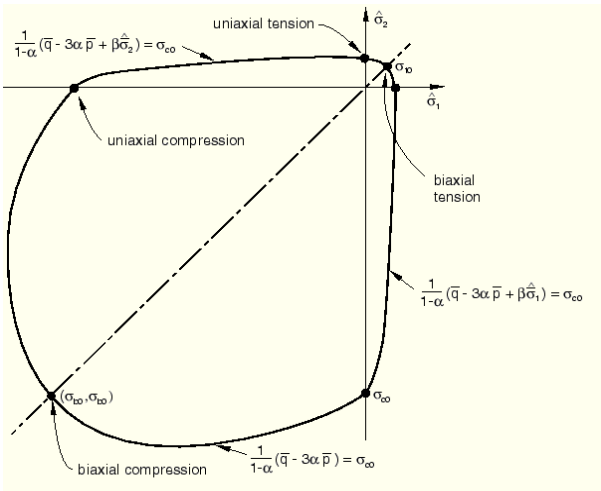

Figure 6: Yield surfaces in the plane stress as presented by [4]

TABLE 1. MODELLING PARAMETER BY [2]

Dimension (mm)	Type of loading	Biaxial ratio σ_1	Biaxial ratio σ_2	Poisson's ratio (MPa)
200×200×50	Compression	-1	0	0.2
		-1	-1	
		-1	-0.52	
	Tension	-1	0	0.18
		-1	1	
		-1	0.55	
	Compression - Tension	-1	0	0.19
		-1	0.052	
		-1	0.103	
		-1	0.204	

TABLE 2. MODELLING PARAMETER BY [3]

Dimension (mm)	Type of loading	Biaxial ratio σ_1	Biaxial ratio σ_2	Poisson's ratio (MPa)
150×150×50	Compression	-1	0	0.22
		-1	-1	
		-1	-0.5	
		-1	-0.2	

TABLE 3. INPUT PARAMETERS FOR CONCRETE DAMAGE PLASTICITY USING ABAQUS SOFTWARE

Dilatation angle	Flow potential eccentricity	Biaxial / Uniaxial stress ratio	Deviatoric stress invariant ratio	Viscosity parameter
15	0.1	1.16	0.67	0

TABLE 4. SIMULATION RESULTS OF PROPOSED MODELS SUBJECTED TO BIAXIAL COMPRESSIONS BASED ON EXPERIMENTAL STUDY BY [2]

Model	Peak Stress σ_1			Peak Strain ε_1		
	Experiment	Model	Ratio	Experiment	Model	Ratio
KP1	-32.06	-30.61	0.955	-0.00206	-0.00225	1.093
KP2	-37.00	-36.90	0.997	-0.00249	-0.00223	0.895
KP3	-40.27	-41.48	1.030	-0.00310	-0.00246	0.793
Average	0.994065			0.927134		
SDV	0.012620			0.050972		
Model	Peak Stress σ_2			Peak Strain ε_2		
	Experiment	Model	Ratio	Experiment	Model	Ratio
KP1	-32.06	-30.61	0.955	0.00084	0.00107	1.269
KP2	-37.00	-36.90	0.997	-0.00249	-0.00223	0.895
KP3	-40.27	-41.48	1.030	-0.00079	-0.00136	1.718
Average	0.994065			1.293974		
SDV	0.012620			0.137341		
Model	Peak Stress σ_3			Peak Strain ε_3		
	Experiment	Model	Ratio	Experiment	Model	Ratio
KP1	-32.06	-30.61	0.955	0.00084	0.00107	1.269
KP2	-37.00	-36.90	0.997	0.00333	0.00290	0.871
KP3	-40.27	-41.48	1.030	0.00200	0.00212	1.058
Average	0.994065			1.066025		
SDV	0.012620			0.06286		

TABLE 5. SIMULATION RESULTS OF PROPOSED MODELS SUBJECTED TO BIAXIAL COMPRESSIONS BASED ON EXPERIMENTAL STUDY BY [3]

Model	Peak Stress σ_1			Peak Strain ε_1		
	Experiment	Model	Ratio	Experiment	Model	Ratio
YN1	-37.60	-37.61	1.000	-0.00210	-0.00300	1.431
YN2	-46.62	-46.63	1.000	-0.00181	-0.00408	2.256
YN3	-49.18	-49.91	1.015	-0.00298	-0.00326	1.092
YN4	-55.05	-55.11	1.001	-0.00337	-0.00372	1.103
Average	1.004063			1.470491		
SDV	0.001792			0.136722		

Model	Peak Stress σ_2			Peak Strain ε_1		
	Experiment	Model	Ratio	Experiment	Model	Ratio
YN1	-37.60	-37.61	1.000	0.00140	0.00097	0.693
YN2	-46.62	-46.63	1.000	-0.00215	-0.00408	1.899
YN3	-49.18	-49.91	1.015	0.00112	0.00095	0.845
YN4	-55.05	-55.11	1.001	-0.00048	-0.00108	2.243
Average	1.004063			1.420095		
SDV	0.001792			0.191804		

Model	Peak Stress σ_3			Peak Strain ε_1		
	Experiment	Model	Ratio	Experiment	Model	Ratio
YN1	-37.60	-37.61	1.000	0.00084	0.00107	1.269
YN2	-46.62	-46.63	1.000	0.00333	0.00290	0.871
YN3	-49.18	-49.91	1.015	0.00200	0.00212	1.058
YN4	-55.05	-55.11	1.001	0.00226	0.00261	1.157
Average	1.004063			1.392268		
SDV	0.001792			0.245915		

TABLE 6. SIMULATION RESULTS OF PROPOSED MODELS SUBJECTED TO BIAXIAL TENSIONS BASED ON EXPERIMENTAL STUDY BY [2]

Model	Peak Stress σ_1			Peak Strain ε_1		
	Experiment	Model	Ratio	Experiment	Model	Ratio
KP4	2.61	2.60	0.998	0.0000916	0.0000800	1.431
KP5	2.61	2.56	0.981	0.0000732	0.0000787	2.256
KP6	2.66	2.58	0.970	0.0000780	0.0000795	1.092
Average	0.982799			0.989157		
SDV	0.004644			0.034697		
Model	Peak Stress σ_2			Peak Strain ε_1		
	Experiment	Model	Ratio	Experiment	Model	Ratio
KP4	2.61	2.60	0.998	-0.0000156	-0.0000104	0.667
KP5	2.61	2.56	0.981	0.0000732	0.0000770	1.052
KP6	2.66	2.58	0.970	0.0000296	0.0000330	1.115
Average	0.982799			0.944481		
SDV	0.004644			0.080882		
Model	Peak Stress σ_3			Peak Strain ε_1		
	Experiment	Model	Ratio	Experiment	Model	Ratio
KP4	2.61	2.60	0.998	-0.0000156	-0.0000104	0.667
KP5	2.61	2.56	0.981	-0.0000308	-0.0000260	0.844
KP6	2.66	2.58	0.970	-0.0000260	-0.0000220	0.846
Average	0.982799			0.785659		
SDV	0.004644			0.034352		

TABLE 7. SIMULATION RESULTS OF PROPOSED MODELS SUBJECTED TO BIAXIAL COMPRESSION-TENSION BASED ON EXPERIMENTAL BY [2]

Model	Peak Stress σ_1			Peak Strain ε_1		
	Experiment	Model	Ratio	Experiment	Model	Ratio
KP7	-32.06	-30.6054	0.955	-0.00206	-0.00225	1.093
KP8	-27.25	-27.5514	1.011	-0.00125	-0.00131	1.045
KP9	-19.88	-20.0902	1.011	-0.00086	-0.00077	0.900
KP10	-12.02	-12.9926	1.081	-0.00044	-0.00040	0.909
Average	1.014265			0.986910		
SDV	0.012903			0.024316		
Model	Peak Stress σ_2			Peak Strain ε_1		
	Experiment	Model	Ratio	Experiment	Model	Ratio
KP7	-32.06	-30.6054	0.955	0.00084	0.00085	1.010
KP8	-27.25	-27.5514	1.011	0.00056	0.00042	0.757
KP9	-19.88	-20.0902	1.011	0.00045	0.00039	0.876
KP10	-12.02	-12.9926	1.081	0.00022	0.00022	1.000
Average	1.014265			0.910556		
SDV	0.012903			0.029839		
Model	Peak Stress σ_3			Peak Strain ε_1		
	Experiment	Model	Ratio	Experiment	Model	Ratio
KP7	-32.06	-30.6054	0.955	0.00084	0.00159	1.891
KP8	-27.25	-27.5514	1.011	0.00040	0.00043	1.065
KP9	-19.88	-20.0902	1.011	0.00017	0.00013	0.758
KP10	-12.02	-12.9926	1.081	0.00008	0.00008	1.000
Average	1.014265			1.178491		
SDV	0.012903			0.123185		